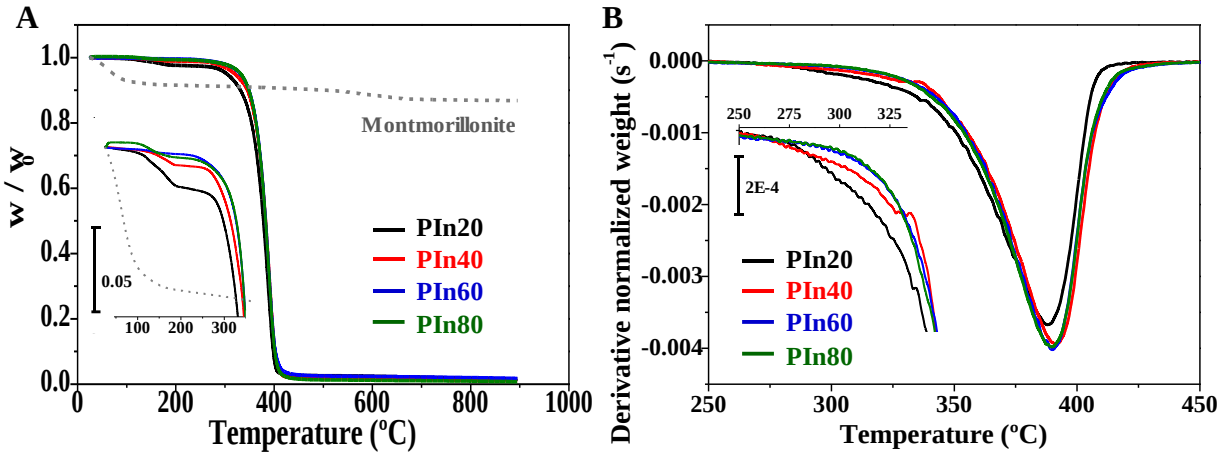

Figure 1. Normalized (A) TG and DTG (B) curves of the PIns prepared at different

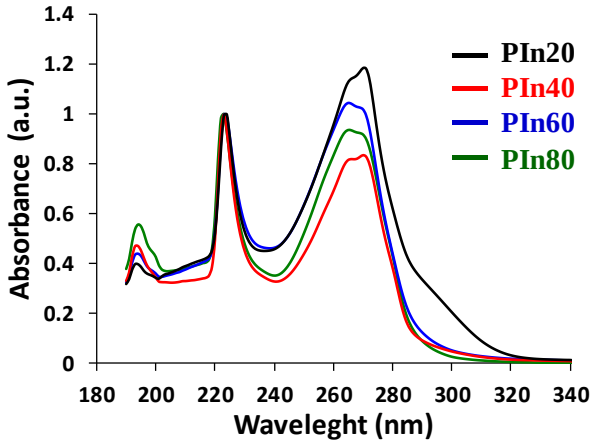

Figure 2. UV absorption spectra of PIns prepared at different temperatures.

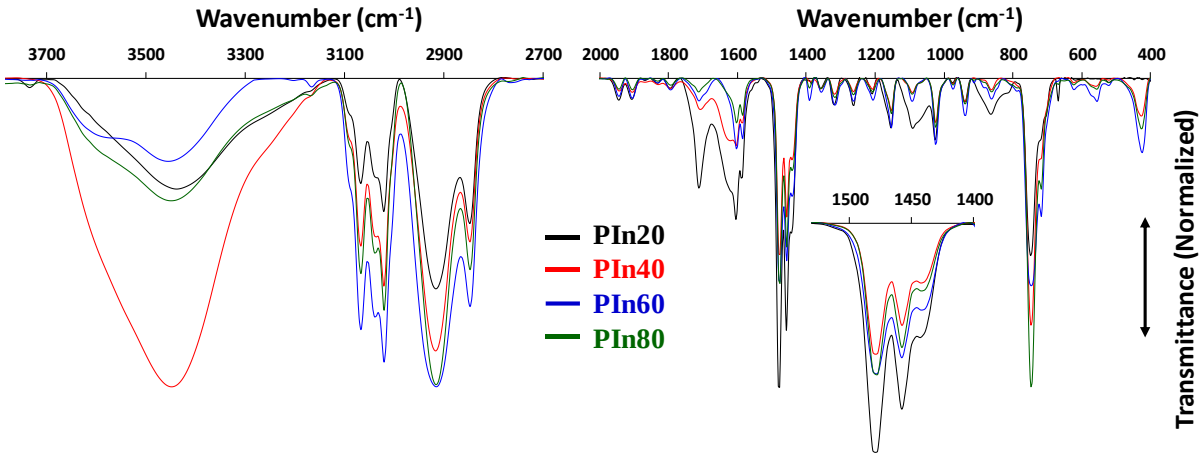

Figure 3. FTIR transmittance spectra of the polyindenes prepared at different temperatures.

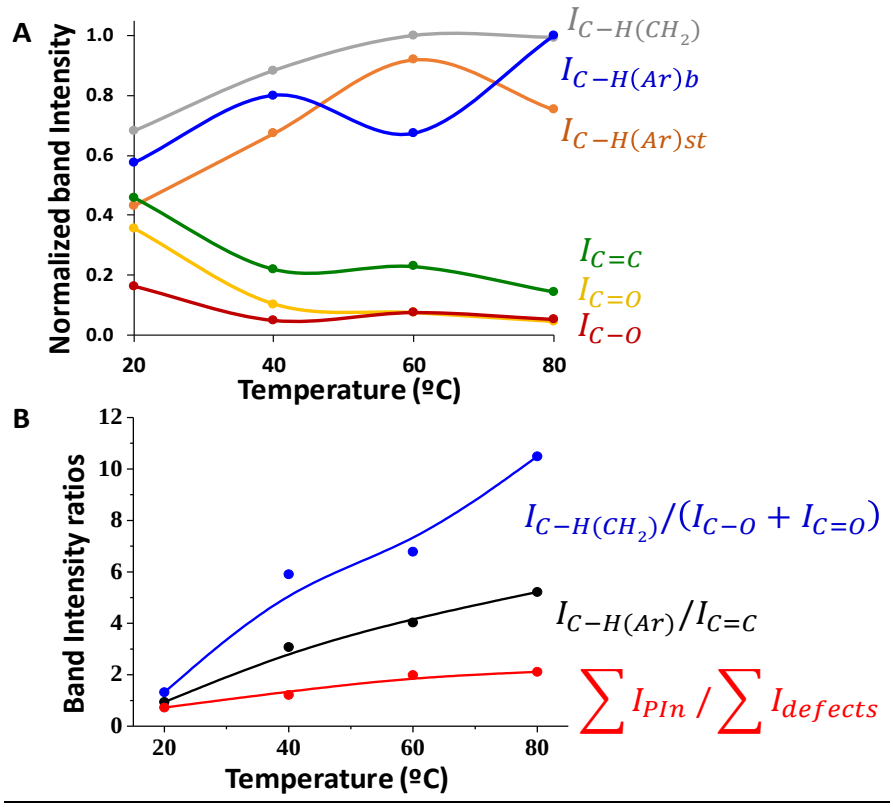

Figure 4. Effect of the synthetic temperature on the intensity of main IR bands (A), and on the ratio of some IR bands (B). Note : $I_{C-H(Ar)} = I_{C-H(Ar)st} + I_{C-H(Ar)b}$; $\sum I_{PIn} = I_{C-H(Ar)} + I_{C-H(CH2)}$; $\sum I_{defects} = I_{C=C} + I_{C-O} + I_{C=O}$.

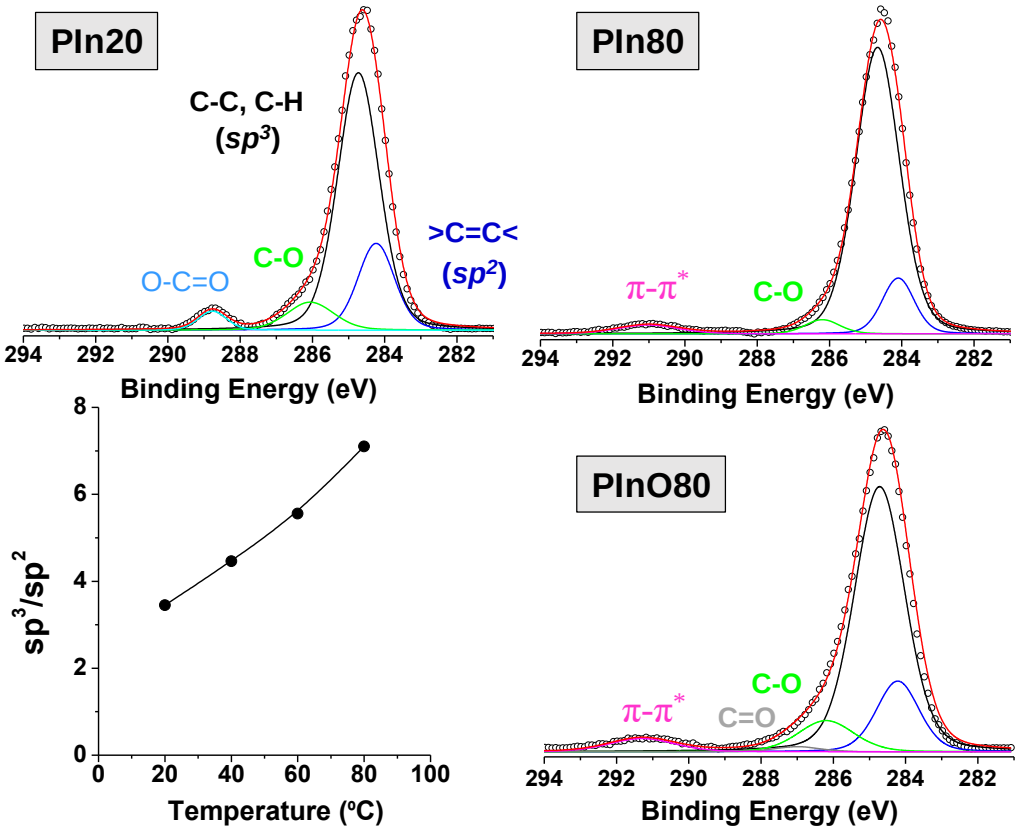

Figure 5. C(1s) XPS spectra of different polyindenes (PIn20, PIn80 and PInO80) and the effect of the reaction temperature on the relative contribution of sp^3 to sp^2 hybridizations.

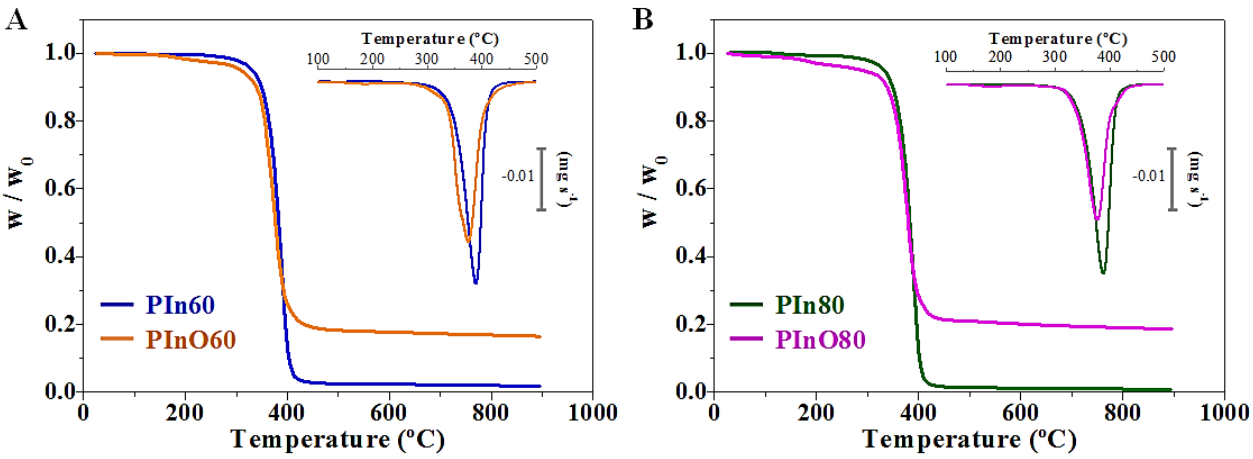

Figure 6. Normalized TG curves of PIn60 (A) and PIn80 (B) samples before and after oxidation. Inlet: DTG curves of the samples.

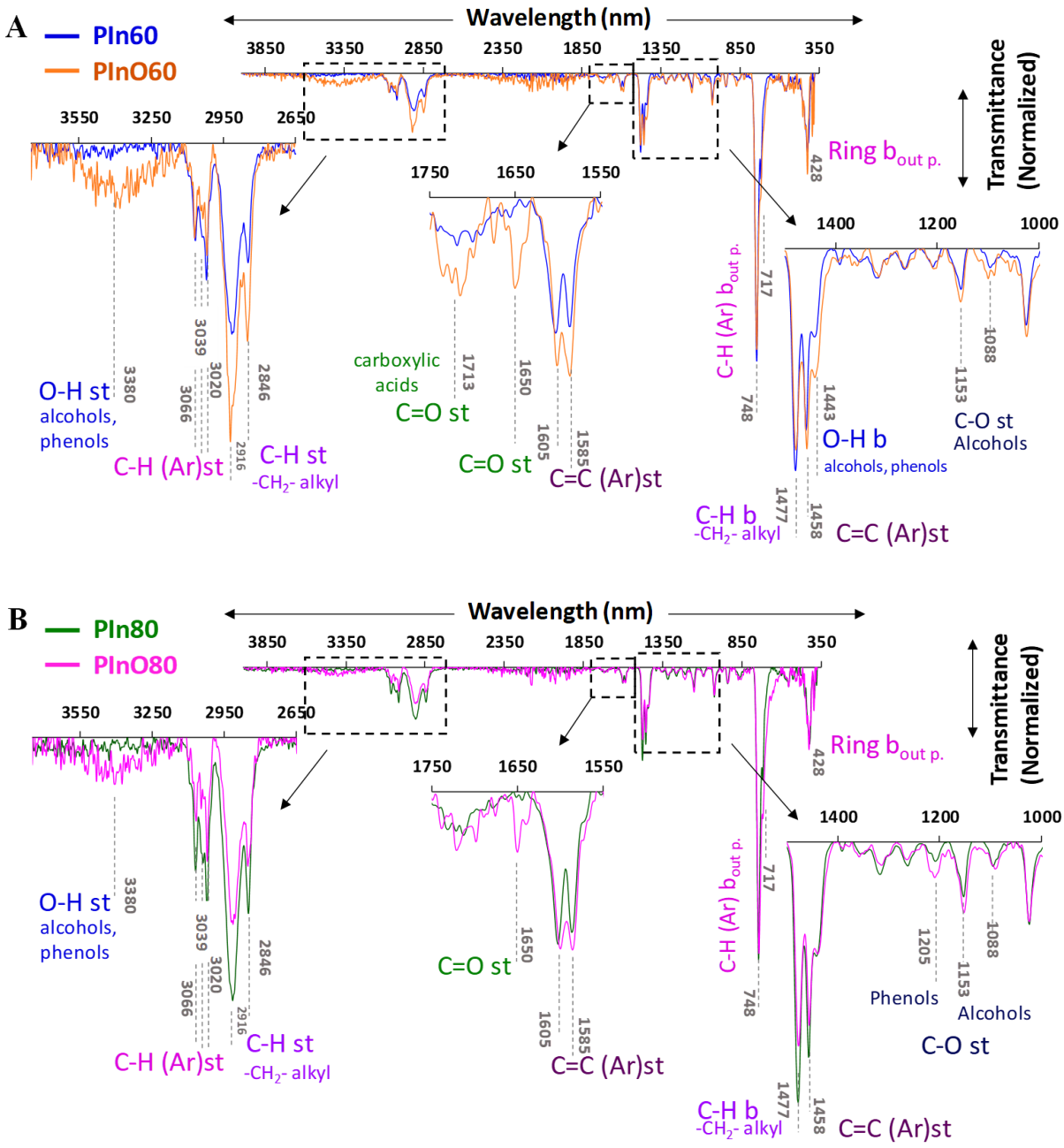

Figure 7. FT-IR spectra of PIns prepared at 60 and 80 ºC and their respective oxidized products.

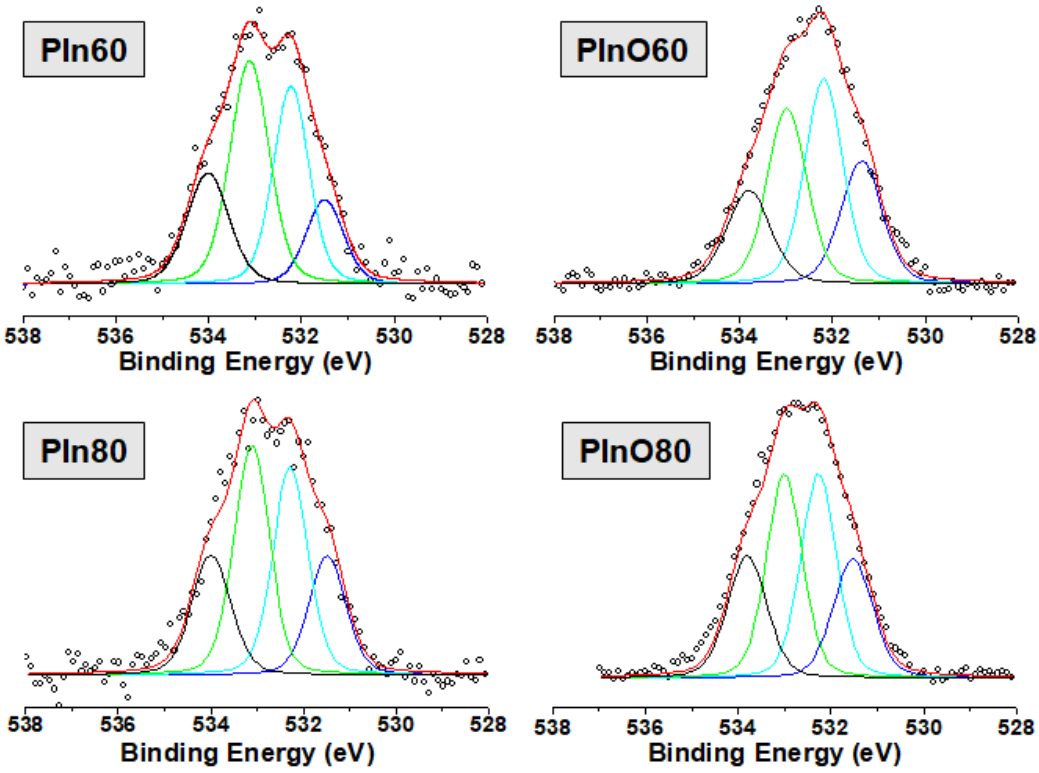

Figure 8. O(1s) XPS spectra of the polyindenes PIn60 and PIn80 before and after treatment with $FeCl_3$.

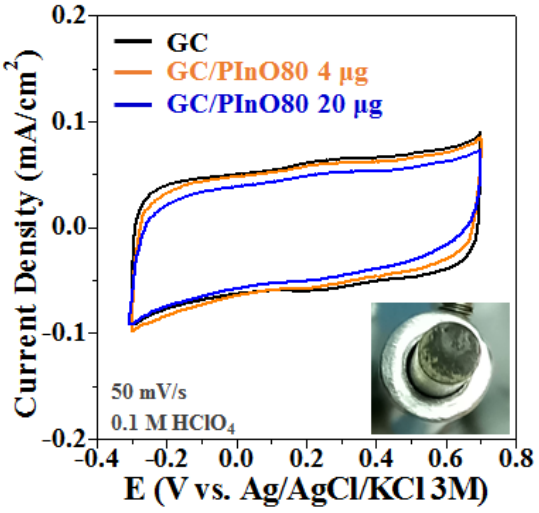

Figure 9. Steady-state cyclic voltammograms of a glassy carbon electrode before and after deposition of different amounts of the PInO80 sample. Inlet: photo of the tip of the GC bar with a deposit of 4 µg of PInO80 after electrochemical analysis.